



## HIGH TEMPERATURE OXIDATION BEHAVIOUR OF MATERIALS FOR SUPERCRITICAL FOSSIL FUEL POWER PLANT IN AIR AND O<sub>2</sub> + WATER VAPOUR ENVIRONMENTS

**P.Mathiazhagan and A.S. Khanna**

*Corrosion Science and Engineering  
Indian Institute of Technology Bombay, Mumbai - 400076*

### ABSTRACT

In recent years a new group of ferritic stainless steels has been developed for supercritical fossil fuel power plant with chromium contents between 9 to 12%. These steels (P9, P91, P92 and E911) are nowadays widely used in the advanced power plants. These steels have excellent mechanical properties and creep resistance with high thermal fatigue life, as well as with good thermal conductivity and resistance to corrosion. However, the corrosion resistance in water vapour/ steam is not upto the mark and needs further evaluation for being suitable for present application. Oxidation behaviour of these materials has been studied. The experiments have been carried out in air and O<sub>2</sub>+5.6%H<sub>2</sub>O environments conditions at the temperature range of 600°C to 800°C. The oxidation kinetics of these alloys shows parabolic behaviour in air due to the formation of protective oxide scale at 600°C. At 700°C, the weight gain of E911 alloy was less compared to P9, P91 and P92 alloys. After 67 hours the alloy shows breakaway oxidation, due to the formation of oxide rosettes. When the oxidation temperature was increased to 800°C, the alloys P91, P92, E911 show breakaway in short duration of exposure and changed to linear oxidation. In O<sub>2</sub>+5.6%H<sub>2</sub>O condition the alloys P9, P91, P92 and E911 show parabolic behaviour at 600°C. However at 700°C, the alloy P92 shows higher oxidation rate due to the depletion of chromium beneath the oxide scale of the alloy, scales cracks are developed and chromium is internally oxidized, under these conditions the oxidation rate increases significantly. The oxide scales are characterized using SEM, XRD and EDAX technique respectively.

**Keywords:** 9 to 12% steels, high temperature oxidation, SEM, XRD.

### 1. INTRODUCTION

Supercritical fossil fuel power plants with efficiencies of 45% have much lower emissions than subcritical plants for a given power output<sup>1</sup>. Steam temperature is a key factor, which controls the plant efficiency and the emission gas. Increasing the steam operating temperature and pressure will proportionally increase the plant efficiency with reduction in the emission gas. Materials used in the power plant should withstand against creep and steam oxidation, with increase in the steam operating temperature<sup>2</sup>. The most modern fossil fuel power plant now in operation, reaches efficiencies of around 42% with steam temperatures of 600° C and pressures of 250 to 300 bar. The next generation of steam power plant should be capable of operating with steam temperatures at 625 to 650 °C, to enable thermal efficiencies of around 45% to be achieved<sup>3</sup>. An increase in the steam temperature from common 535 to 650°C and the steam pressure from 185 to 300 bar would enable a reduction in fuel consumption and a reduction of CO<sub>2</sub> emission by more than 25%<sup>4</sup>. To allow these increases, advanced materials are needed that are able to withstand the higher temperatures and pressures in terms of strength, creep, and oxidation resistance<sup>5</sup>. In recent years a new group of ferritic stainless steels has been developed

with chromium contents between 9 to 12%. Typical representatives of these steels are P9, P91, P92 and E911, which are nowadays widely used in the supercritical power plants. These steels possess excellent oxidation resistance during service in oxygen or air. It is well known that in the presence of water vapour, as prevailing under power plant conditions, the oxidation rates of these alloys are significantly enhanced<sup>6</sup>. As indicated by several publications, the water vapour content in the environment which has a particular influence on kinetics and scale structure during oxidation of these alloys. Taking all these aspects into consideration the present work involves study of oxidation in air and  $O_2+5.6\%H_2O$  environments condition under isothermal exposure at 600 to 800 °C. The oxidation rate kinetics are presented and subsequently explained on the basis of morphology and composition of the oxide layers formed on the surface.

## 2. MATERIALS

The P9, P91 and P92, E911 alloys were supplied by Indira Gandhi Centre for Atomic Research, Kalpakkam, India and Forschungszentrum Julich, Germany. The P9, P91 and P92, E911 samples, received in the form of 250x250x12 mm thick plate and 30mm diameter rod, were cut into 10x 5x 2mm thickness in size. The chemical compositions of the alloys were determined with the inductively coupled plasma (ICP –AES) technique and are tabulated in table 1.

The samples were mechanically polished on silicon carbide (SiC) papers with a fine roughness of 1200 grit, washed and subsequently cleaned in acetone. The surface area of samples were measured with a digimatic caliper (Mitutoyo) and weighed on a precision balance (Sartorius) before performing the oxidation experiments.

## 3. EXPERIMENTAL

### 3.1 Thermogravimetry

The Linseis L81 Thermobalance was used for thermogravimetric analyses; continuous change in weight was registered as a function of time to obtain the kinetics of the oxidation. The oxidation tests were carried out in atmospheric air at 600, 700 and 800 °C. For all the experiments a ramp-heating program with a heating rate of 20°C/min was used to reach the desired temperature.

### 3.2 Steam Oxidation

For steam oxidation the experimental facility used is shown in fig (1). The samples were oxidized in a horizontal furnace fitted with a (32mm) diameter Quartz glass tube.

The samples were mounted in alumina boat which was introduced in horizontal reaction tube and samples were positioned parallel to the direction of gas flow. The reaction atmosphere of ( $O_2+5.6\%H_2O$ ) gas mixture was obtained by bubbling purified  $O_2$  (99.999 % pure) gas through saturator (water flask) containing distilled water. The distilled water temperature was thermostatically controlled at  $35 \pm 1^\circ C$ , producing a water vapour concentration of 5.6%. At this temperature, vapour pressure of water is 0.05628 bar. The furnace is equipped with a PID (Proportional Intergral and Derivative) controller to control the temperature at 600 to 800°C. The mass changes were recorded at definite interval using a precision balance to obtain oxidation kinetics.

## 4. RESULTS

### 4.1. Kinetics of oxidation

Figs. 2-4 shows the continuous weight change data of the P9, P91, P92 and E911 alloys at the temperature range of 600 to 800 °C in air upto 99 hours. The results indicate that all the alloys show parabolic kinetics at the temperature range of 600°C due the formation protective (FeO.Cr<sub>2</sub>O<sub>3</sub>) oxide scale. The alloys P9 and P91 shows high and low weight gain compared with the other two alloys (P92 and E911) at 600 °C. At 700°C, the weight gain of E911 alloy was less compared to P9, P91 and P92 alloys. After 67 hours the alloy shows breakaway oxidation, due to the formation oxide rosettes.

At this point the oxide scale started to fail usually due to crack formation. When the oxidation temperature was increased to 800°C, the alloys P91, P92, E911 shows breakaway oxidation in short duration of exposure and changed to linear oxidation.

However the alloy P9 shows less weight gain and follows parabolic kinetics. The parabolic rate constants (Kp) measured by plotting the square of weight gain as a function of exposure time, showed increasing values of the constants with increasing temperature except P9 alloy at 700 to 800 °C. The values of (Kp) are  $2 \times 10^{-6}$ ,  $1 \times 10^{-6}$ ,  $1 \times 10^{-6}$  (P9 alloy),  $7 \times 10^{-7}$ ,  $3 \times 10^{-6}$ ,  $4 \times 10^{-5}$  (P91 alloy),  $5 \times 10^{-7}$ ,  $2 \times 10^{-6}$ , 0.0003 (P92 alloy) and  $1 \times 10^{-6}$ ,  $4 \times 10^{-6}$ , 0.0004 (E911 alloy) ( $\text{mg}^2/\text{mm}^4 \text{ hr}^{-1}$ ) at 600 to 800°C. The weight change vs time curves in Figs 5-7 describes the oxidation behaviour of P9, P91, P92 and E911 alloys in O<sub>2</sub> +5.6% H<sub>2</sub>O environment at 600 to 800 °C up to 300 hours. The P92 and E911 alloys clearly exhibit increasing oxidation rates with increasing temperature. The P92 alloy exhibit higher weight gain compared to other three alloys and all these alloys shows parabolic behaviour at 600 °C. The weight gains of P91 and E911 alloys almost same at this temperature. At 700 °C, the alloy P92 shows breakaway oxidation after short duration of exposure and changes to linear oxidation due to the formation of non-protective oxide. The P9 alloy shows less weight gain due to the higher silicon content at this temperature. Silicon seems to have a beneficial effect in water containing environments with regard to slowing down the chromium depletion rates in the metal subsurface zone and thus, extending the time to breakaway oxidation significantly<sup>7</sup>.

At 800 °C the P92 and E911 alloys shows higher oxidation rate throughout the exposure time. However the P9 and P91 alloys shows less weight gain and follows parabolic behaviour. The parabolic rate constants (Kp) measured by plotting the square of weight gain as a function of exposure time. The values of (Kp) are  $4 \times 10^{-7}$ ,  $4 \times 10^{-7}$ ,  $4 \times 10^{-7}$  (P9 alloy),  $6 \times 10^{-7}$ ,  $7 \times 10^{-7}$ ,  $3 \times 10^{-8}$  (P91 alloy),  $4 \times 10^{-6}$ ,  $6 \times 10^{-5}$ , 0.0005 (P92 alloy) and  $4 \times 10^{-7}$ ,  $2 \times 10^{-5}$ ,  $9 \times 10^{-5}$  (E911 alloy) ( $\text{mg}^2/\text{mm}^4 \text{ hr}^{-1}$ ) at 600 to 800°C.

### 4.2. XRD Analysis

Fig. 8 -10 show the X- ray diffraction result carried out on the oxide scale without disturbing the oxidized. The FeO.Cr<sub>2</sub>O<sub>3</sub> oxide was formed at 700 °C of P92 and E911 alloys. When the temperature was increased to 800 °C, the mixed oxide (FeO.Cr<sub>2</sub>O<sub>3</sub>) changes to spinel oxide FeCr<sub>2</sub>O<sub>4</sub>. Fe<sub>2</sub>O<sub>3</sub> was found to be the dominant outmost oxide. In O<sub>2</sub>+5.6%H<sub>2</sub>O environment conditions the spinel oxide FeCr<sub>2</sub>O<sub>4</sub> was formed at 600 °C on P9, P91 and P92 alloys. However at 700 °C, spinel changes to mixed oxide (FeO.Cr<sub>2</sub>O<sub>3</sub>) and FeCr<sub>2</sub>O<sub>4</sub> formed internally. The intensity of FeCr<sub>2</sub>O<sub>4</sub> was reduced due to the presence of water vapour content and hematite (Fe<sub>2</sub>O<sub>3</sub>) formed as an outmost oxide at 700°

### 4.3. Surface morphology analysis

Detailed oxide scale characterization was carried out on the scales formed after various temperature of oxidation. Fig.11-13 shows SEM morphology of the scale surfaces formed on the alloy after exposure at different temperatures in the range of 600 to 900°C in air. A thick and uniform oxide scale was developed on the sample treated at 600 to 700°C of P92 alloy. When the oxidation temperature was increased to 800 °C, the uniform oxide changes to nodule type oxide. At 900 °C, crack formation was observed. The cracks (Fig 11 (d)) are likely to be related to stresses originating from thermal expansion coefficient between alloy and oxide at this temperature, the thermal expansion coefficient of magnetite ( $\text{Fe}_3\text{O}_4$ ) being larger than that of alloy

A thin oxide scale was developed on E911 alloy treated at 600 °C. At 700 °C, the thin oxide changes to oxide rosettes, such a situation lead to breakaway oxidation. This was observed in thermogravimetric result as shown in fig (3). Fig 12-13 shows morphology of three alloys (P91, P92 and E911) under ( $\text{O}_2+5.6\%\text{H}_2\text{O}$ ) environment conditions at the temperature range of 600 to 700 °C. A thin and thick uniform oxide scale were formed on both alloys (P91 and E911) at 600 to 700 °C. At 600°C, the oxide exhibits a needle type growth of alloy P92 and crack observed at 700 °C. Thus, this structure leads to non-protective oxide and increased the oxidation rate.

## 5. DISCUSSIONS

The oxidation behaviour of these alloys depends mainly on temperature, length of oxidation and environment conditions. A comparison study of these alloys in atmospheric air in the temperature range of 600 to 800 °C reveals some differences in their oxidation kinetics, due to the higher chromium content of P9 and P91 alloys. At 700°C, the alloy E911 shows breakaway oxidation after 67 hours, due to the formation oxide rosettes. The P92 alloy shows higher weight gain at 600°C compared to other three alloys due to depletion of chromium from substrate under  $\text{O}_2+5.6\%\text{H}_2\text{O}$  environment conditions. This is confirmed by EDAX technique. At 700 °C, the alloy P92 shows breakaway oxidation after short duration of exposure and changes to linear oxidation due to the formation of cracks and spallation in the oxides. The P9 alloy shows less weight gain at 800°C due to the higher silicon content. Silicon seems to have a beneficial effect in water containing environments with regard to slowing down the chromium depletion rates in the metal subsurface zone and decrease the oxidation rate.

## 6. CONCLUSION

Steam oxidation study was conducted at the temperature of 600 to 800°C upto 300 hours in ( $\text{O}_2+5.6\%\text{H}_2\text{O}$ ) environment. Short-term kinetic studies were also carried out over the temperature range 600 to 800°C for 99 hours using thermogravimetric analyzer. The following results were obtained.

1. At 600 to 700°C, the alloys P9, P91 and P92 shows parabolic behaviour throughout the exposure time in air. Whereas at 700 °C the alloy E911 show parabolic behaviour up to 67 hours and it changes to breakaway oxidation. This behaviour is due to the formation oxide rosettes.
2. At 800°, the alloys P91, P92, E911 shows breakaway oxidation in short duration of exposure and changed to linear oxidation. . However the alloy P9 shows less weight gain and follows parabolic kinetics.
3. At 600 to 700°C, the alloys P9, P91 and E911 shows parabolic behaviour throughout the exposure time in  $\text{O}_2+5.6\%\text{H}_2\text{O}$  environment conditions. However at 700°C, the alloy P92 show breakaway oxidation and changes to linear after 60 hours duration of exposure. This behaviour is due to effect of water vapour content present in the test gas.

4. The P9 alloy shows less weight gain at 800°C due to the higher silicon content. Silicon seems to have a beneficial effect in water containing environments with regard to slowing down the chromium depletion rates in the metal subsurface zone and decrease the oxidation rate
5. At 800°C, the alloys P92 and E911 shows higher oxidation rate due to the formation of non-protective oxides were formed on the surface.

## REFERENCES

1. Ingo Paul, *Energy Issues*, (19) (1999).
2. T. Sundararajan, S. Kuroda, T. Itagaki and F. Abe, *The J of Corrosion Science and Engineering* (1 6) (H050)
3. P.J. Ennis and A. Czyrska –Filemonowicz, *OMMI* (1) (2002)
4. J. Zurek, E. Wessel, L. Niewolak, F. Schimtz, T. U. Kern L. Singheiser, W.J. Quadackers, *Corrosion science* 46 (6) (2004) 2301
5. G. R. Holcomb, D. E. Alman, S. B. Bullard, B. S. Covino, Jr., S. D. Cramer and M. Ziomek-Moroz, *Proceeding of 17<sup>th</sup> Annual Conference on Fossil Materials* (2003), NETL Publication.
6. Dionisio Laverde, Tomas Gomez – Acebo, Francisco Castro, *Corrosion Science* 46 (2004) 613
7. M. Schutze, M. Schorr, D. P. Renusch, A. Donchev, J. P. T. Vossen, *Materials Research* 7(1) (2004) 111

## TABLES

Table 1: Chemical compositions of the tested steels (wt %)

Elements	P9	P91	P92	E911
C	0.10	0.10	0.12	.012
Mn	0.53	0.41	0.46	0.54
P	0.024	0.032	0.019	0.019
Cr	9.75	10.12	9.69	9.42
Mo	1.18	1.18	0.47	0.94
Ni	0.18	0.43	0.11	0.31
Si	1.15	0.70	0.059	0.32
S	-	-	0.0228	0.0228
W	-	-	0.014	0.030
V	-	0.1ppm	0.095	0.089
Nb	-	0.1ppm	0.1ppm	0.1ppm
Al	-	-	0.99	-

FIGURES

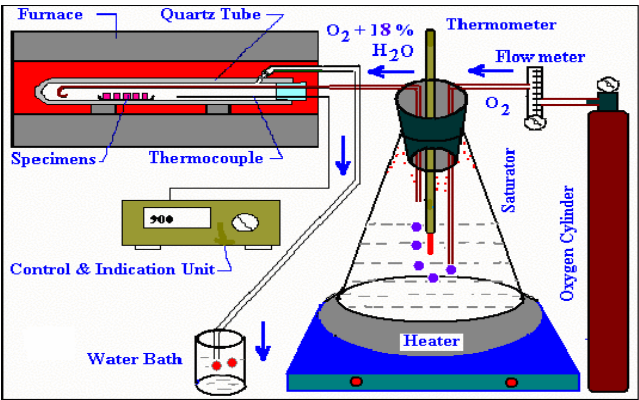


Fig 1: Experimental Set up for Oxidation Test

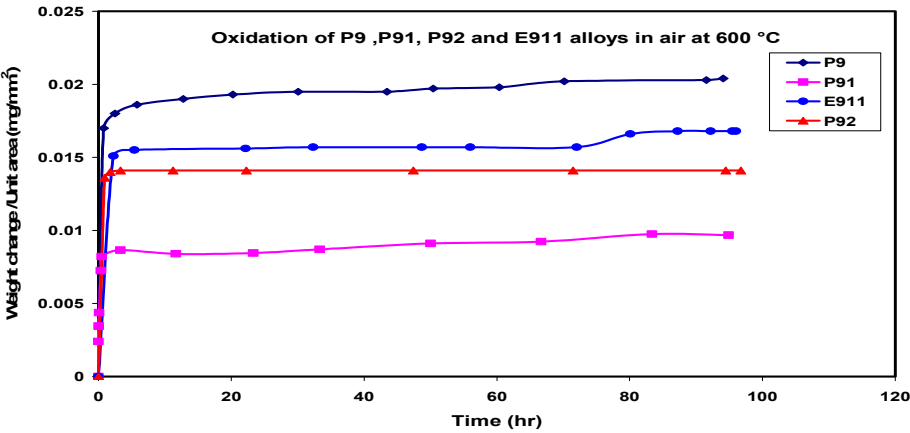


Fig 2 Weight changes of P9, P91, P92 and E911 alloys exposed in air at 600 °C

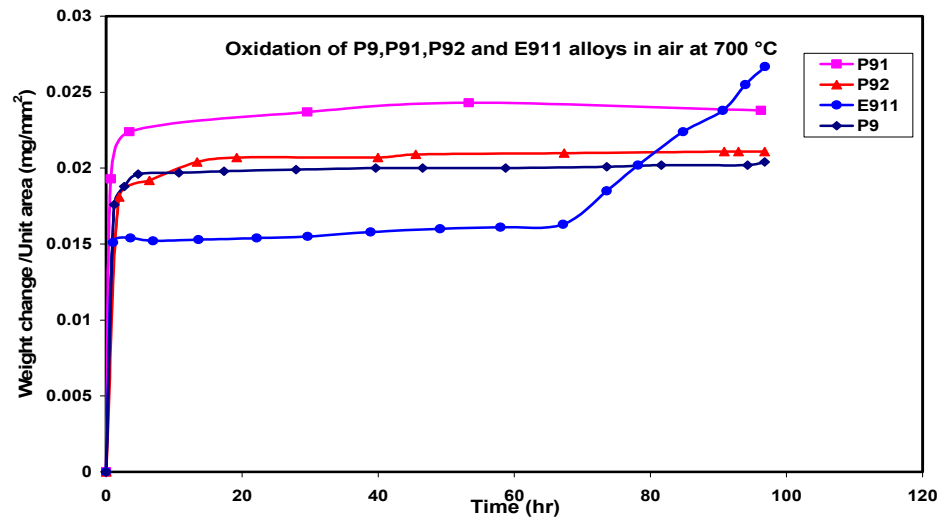


Fig 3 Weight changes of P9, P91, P92 and E911 alloys exposed in air at 700 °C

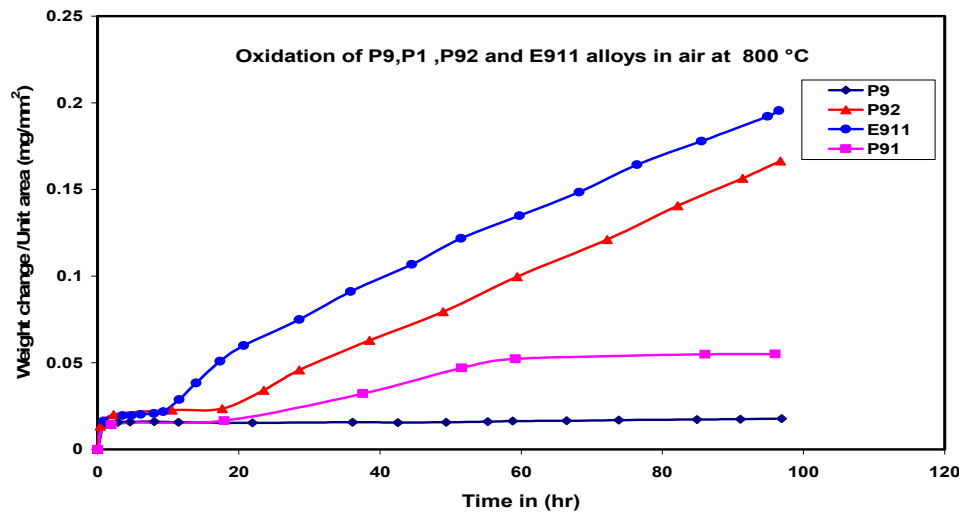
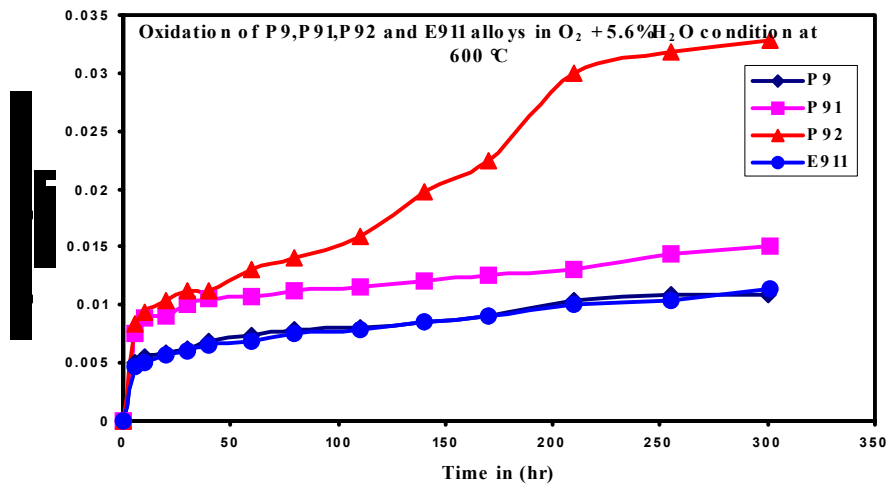
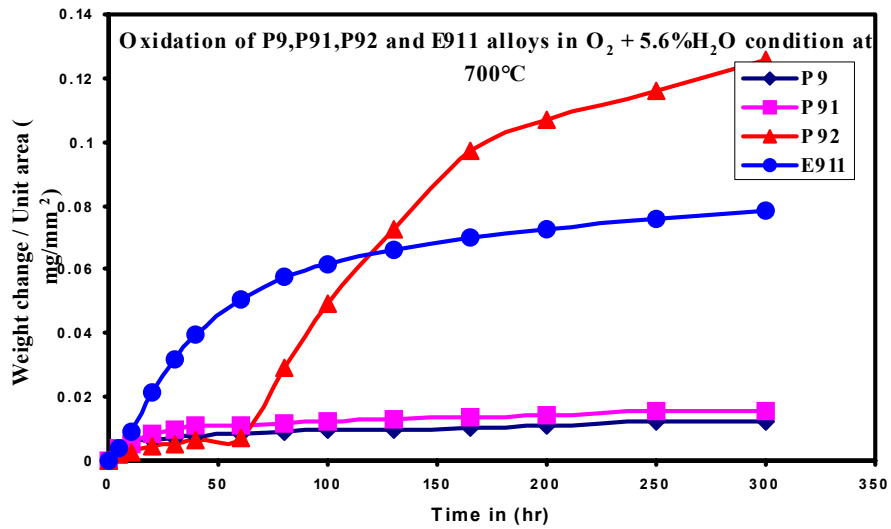
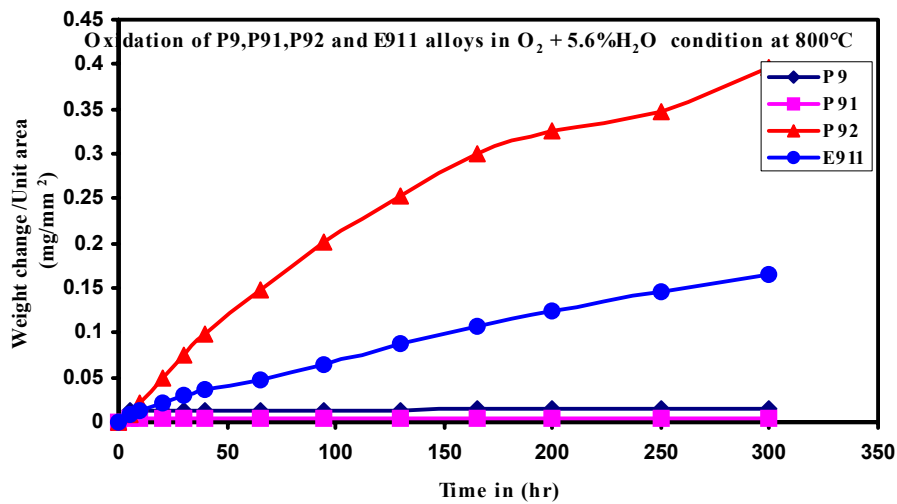


Fig 4 Weight changes of P9, P91, P92 and E911 alloys exposed in air at 800 °C

Fig 5 Weight changes of P9, P91, P92 and E911 alloys in  $O_2 + 5.6\%H_2O$  at 600 °C.Fig 6 Weight change of P9, P91, P92 and E911 alloys in  $O_2 + 5.6\%H_2O$  at 700 °CFig 7 Weight change of P9, P91, P92 and E911 alloys in  $O_2 + 5.6\%H_2O$  at 800 °C.



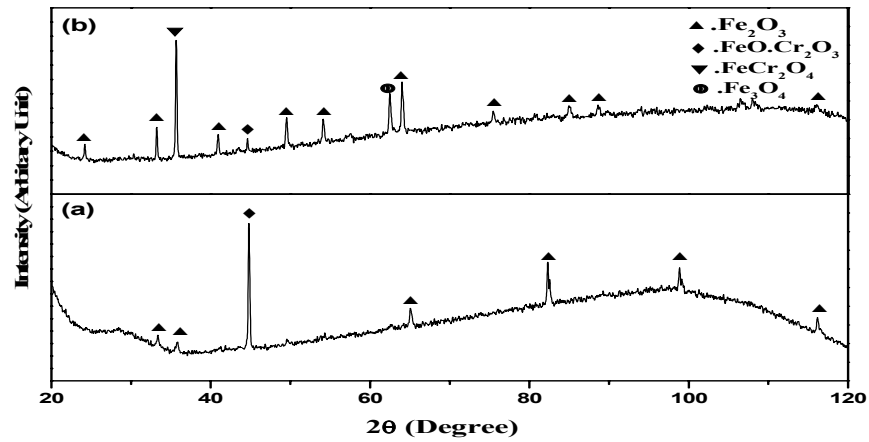


Fig 8 XRD–Pattern of E911 alloy after oxidation in air at (a) 600°C, (b) 700 °C

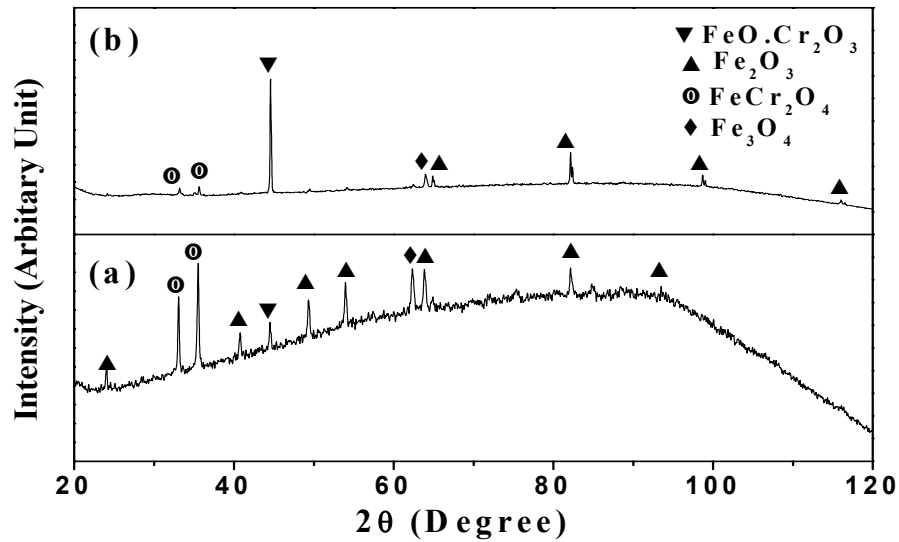


Fig 9 XRD–Pattern of P91 alloy after oxidation in  $\text{O}_2 + 5.6\% \text{H}_2\text{O}$  at (a) 600°C, (b) 700 °C

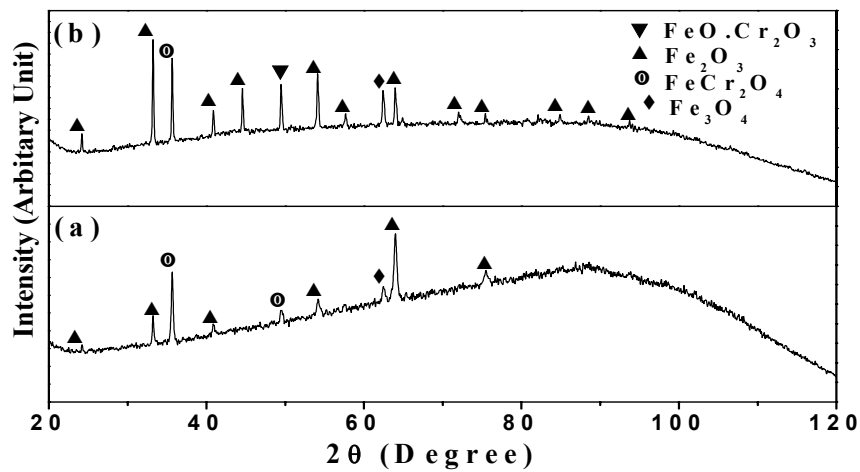


Fig 10 XRD–Pattern of P92 alloy after oxidation in  $\text{O}_2 + 5.6\% \text{H}_2\text{O}$  at (a) 600°C, (b) 700 °C

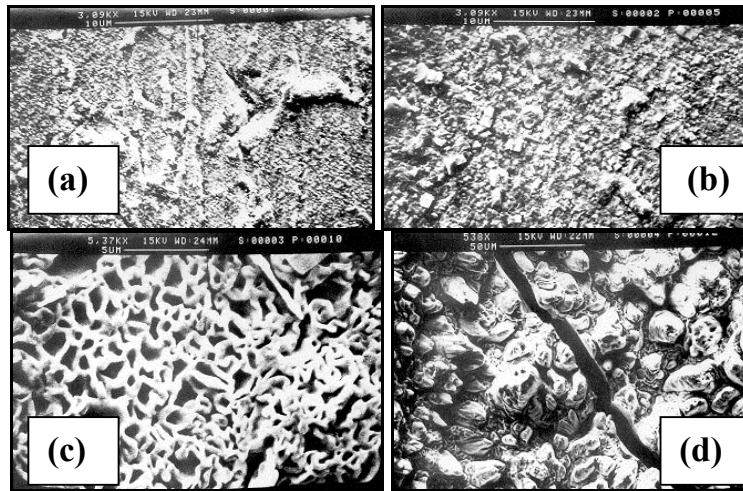


Fig 11 SEM micrographs showing the morphology of oxide layer formed (air) on P92 alloy at (a) 600°C, (b) 700°C, (c) 800°C and (d) 900°C.

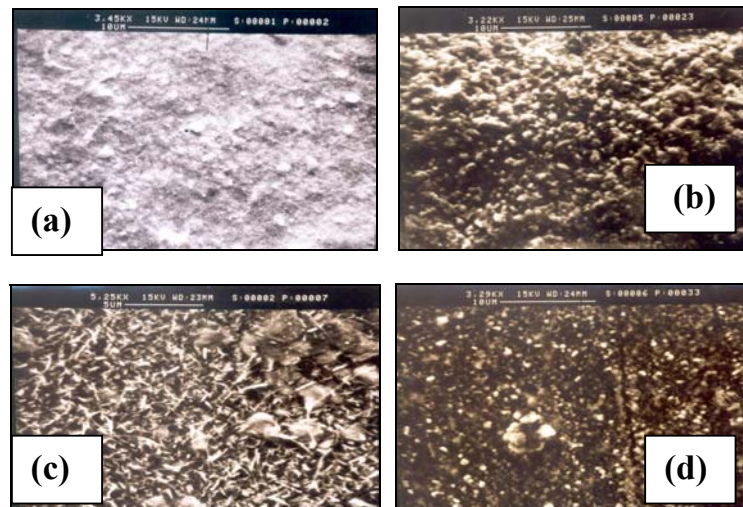


Fig 12 SEM micrographs showing the morphology of oxide layer formed in ( $O_2+5.6\%H_2O$ ) at 600 to 700°C, (a-b) P91 and (c-d) P92 alloys

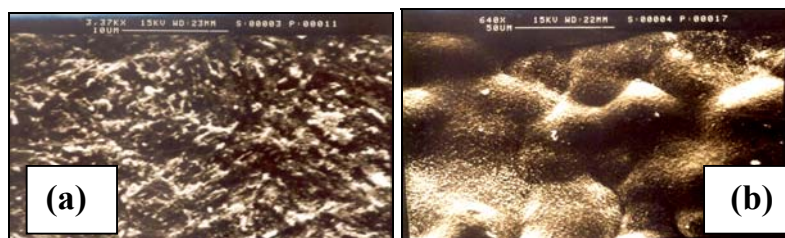


Fig 13 SEM micrographs showing the morphology of oxide layer formed in ( $O_2+5.6\%H_2O$ ) at 600 to 700°C, (a-b) E911 alloys